

Multi-Objective Optimal Power Flow Considering Emissions and Voltage Violations

Jacob Kravits, Kyri Baker, and Joseph Kasprzyk
Civil, Environmental and Architectural Engineering Department
University of Colorado Boulder, Boulder, CO, USA
{jacob.kravits, kyri.baker, joseph.kasprzyk}@colorado.edu

Abstract—In this paper, we propose a novel multi-objective formulation of the environmental/economic optimal power flow (EOPF) problem that considers voltage violations, fuel costs, and emissions as objectives. Traditionally, the EOPF problem only quantified tradeoffs between fuel costs and emissions. This traditional formulation is limiting because it requires analysts to specify numerous constraints before optimization which can be especially problematic if system limits are uncertain or flexible. By considering these constraints as objectives, solutions can be optimized over a larger decision space, and lower cost/emissions can be traded off with potentially small constraint violations. We apply our formulation to the IEEE 30-bus system and use the Borg multi-objective evolutionary algorithm to analyze tradeoffs between objectives. We show that this formulation allows grid operators to apply adjusted constraints after the multi-objective design procedure, thus allowing for greater insights into system performance and further justification of system constraints.

Index Terms—Environmental Optimal Power Flow, Multi-objective Optimization, Evolutionary Algorithm

I. INTRODUCTION

In 2018, the electricity sector contributed 27 percent of the total greenhouse gas emissions in the United States [1]. The concept of considering the environmental impacts in grid operations is not new. Consider the economic dispatch problem. Since the late 1990's and early 2000's there has been a growing amount of literature that takes an environmental view of the economic dispatch problem. Early approaches achieved this by minimizing generation costs and considering environmental impacts as constraints in their problem formulation [2]. Shortly thereafter, the term environmental/economic dispatch (EED) problem was coined to describe a multiple objective approach where emission and fuel costs were both considered objectives in the problem [3]. In contrast to single-objective equivalents of multi-objective problems, where the objectives must be converted to have the same units [4], a multi-objective approach allows us to truly compare objectives such as emissions (ton/hr) with cost (\$/hr) with voltage violations (pu). Such a formulation allows a grid operator to observe the tradeoffs between the objectives to *design* constraint sets, or analyze tradeoff conditions between objectives to yield a “best compromise” solution.

The literature has produced many potential options for solving the EED and environmental optimal power flow (EOPF) problem. Multi-objective mathematical programming, Non-Dominated Sorting Genetic Algorithm (NSGA), NSGA-II, and many other multi-objective evolutionary algorithms (MOEAs)

have been applied to solving these problems [3], [5], [6]. However, these problems were typically formulated as two objective (cost and emission) problems with many constraints such as power balance, generator capacity limits, line limits, and upper/lower voltage limits. New research of the EED has attempted to move some of these constraints to objectives to better analyze tradeoffs within the system. Previous work has added a minimization of total real power loss as a third objective to better observe overall network loss [7]. Building on these studies, we contribute a problem formulation in this paper that includes total voltage violations throughout the network as well as fuel costs and emissions as objectives, while adhering to AC power flow constraints. This problem formulation is tested on the IEEE 30-bus system and the Borg MOEA is implemented to solve the problem [8]. This paper therefore demonstrates how relaxing some of these constraints (and implementing them as objectives) gives operators greater insights into the tradeoffs between constraint relaxation and optimal solutions.

The rest of this paper is organized as follows. Section 2 outlines the multi-objective problem formulation. Section 3 outlines the details of the computational experiment including details about the case study and the Borg MOEA. The results of this paper are then discussed, and the paper is concluded with section 4.

II. PROBLEM FORMULATION

We propose a multi-objective formulation of the EOPF problem that seeks to minimize fuel costs, emissions, and voltage violations by satisfying the AC power flow equations and generation limit constraints. The overall iterative approach is seen in Fig. 1. As seen in the figure, Borg determines candidate generator outputs, which are then evaluated within an AC power flow to determine feasibility and level of voltage violations. The following sections define each component of our problem in more detail.

A. Decisions

Like most traditional economic dispatch and optimal power flow problem formulations, this problem seeks to minimize its objectives by varying the active power produced by each generator P_{Gi} , for all generators $i = 1, \dots, N_G$.

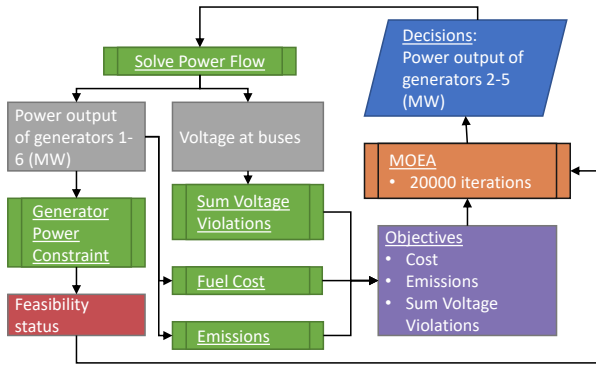


Fig. 1. Overview of optimization routine and information flow

B. Objectives

In this paper, we consider three objectives that are a function of the vector of all active power generation values \mathbf{P}_G and the vector of voltage magnitudes \mathbf{v} .

Minimization of fuel costs: Fuel costs are modeled as a quadratic function of the power generated [3]. These total fuel costs $F(\mathbf{P}_G)$ (\$/hr) are expressed as:

$$F_c(\mathbf{P}_G) = \sum_{i=1}^{N_G} a_i + b_i P_{Gi} + c_i P_{Gi}^2 \quad (1)$$

where \mathbf{P}_G is a vector of all P_{Gi} and a_i , b_i , and c_i are the cost coefficients of the active power output of generator i .

Minimization of emissions: Emission functions are modeled as the sum of all SOx and NOx pollutants for each generator's active power output [3]. These functions have both quadratic and exponential terms. The total emissions $F_e(\mathbf{P}_G)$ (ton/hr) are expressed as:

$$F_e(\mathbf{P}_G) = \sum_{i=1}^{N_G} 10^{-2}(\alpha_i + \beta_i P_{Gi} + \gamma_i P_{Gi}^2) + \xi_i e^{\lambda_i P_{Gi}} \quad (2)$$

where α_i , β_i , γ_i , ξ_i , and λ_i are the emission coefficients of active power output of generator i (power in per unit).

Minimization of total system voltage violations: For a feasible \mathbf{P}_G , there exist a set of feasible voltage magnitudes \mathbf{v} . (see Constraints section). The total amount of voltage violations (in pu) across all the buses $k = 1, \dots, N_b$ is expressed as:

$$F_v(\mathbf{v}) = \sum_{k=1}^{N_b} \max(0, v_k - v_{max}) + \max(0, v_{min} - v_k) \quad (3)$$

where v_k is the voltage magnitude at bus k , and v_{min} and v_{max} are the lower and upper voltage limits, respectively.

C. Constraints

Generator capacity: The generators must generate power within their minimum and maximum limits. This is expressed:

$$P_{Gi}^{min} \leq P_{Gi} \leq P_{Gi}^{max}, i = 1, 2, \dots, N_G \quad (4)$$

where P_{Gi}^{min} and P_{Gi}^{max} are the minimum and maximum active power outputs of generator i , respectively.

Coefficient	G_1	G_2	G_3	G_4	G_5	G_6
a	10	10	20	10	20	10
b	200	150	180	100	180	150
c	100	120	40	60	40	100
α	4.091	2.543	4.258	5.426	4.258	6.131
β	-5.554	-6.047	-5.094	-3.55	-5.094	-5.555
γ	6.49	5.638	4.586	3.38	4.586	5.151
ξ	0.0002	0.0005	0.000001	0.002	0.000001	0.00001
λ	2.857	3.333	8	2	8	6.667

TABLE I
GENERATOR FUEL COST AND EMISSION COEFFICIENTS FROM [3]

D. Problem Formulation

Combining the previous objectives and constraints yields the following multi-objective optimization problem:

$$\begin{aligned} \min_{\mathbf{P}_G} \quad & [F_c(\mathbf{P}_G), F_e(\mathbf{P}_G), F_v(\mathbf{v})] \quad (5) \\ \text{s.t.} \quad & P_{Gi}^{min} \leq P_{Gi} \leq P_{Gi}^{max}, i = 1, 2, \dots, N_G \end{aligned}$$

Note that hard constraints on generator limits are explicitly included in the MOEA, whereas AC power flow feasibility is ensured outside the MOEA.

III. EXPERIMENT AND RESULTS

We test our problem formulation with the IEEE six-generator 30-bus test system and use the Borg MOEA as the multi-objective optimization solver.

A. Computational Experiment

Fuel cost and emissions coefficients shown in Table I have been widely used in previous studies [3], [7], [9]. The minimum and maximum generator capacities P_{Gi}^{min} and P_{Gi}^{max} are set to 5 and 150 MW, respectively, for all $i = 1, \dots, N_G$ [7]. A Newton-Raphson solver with a flat initialization and a maximum of 10 iterations was used to numerically solve the power balance constraints. Voltage bounds v_{min} and v_{max} are 0.95 pu and 1.05 pu, respectively. The test system and default parameters were modeled in the `pandapower` package in Python [10].

B. Borg MOEA

The Borg MOEA [8] used in this work is a search framework that employs multiple search operators. The solution to a multi-objective search problem is a non-dominated tradeoff set. A solution "dominates" another if its performance is better or equal than another solution's performance in all objectives. With high numbers of objectives, there can be a high number of solutions in the tradeoff. The Borg MOEA employs epsilon dominance, user-defined precision on each objective function. Within the dominance calculation, a solution survives only if its performance differences are larger than that epsilon value, limiting the number of solutions found and easing interpretability of tradeoffs.

Epsilon dominance is also employed within the search process as a diagnostic aid. The algorithm keeps track of the number of new epsilon boxes that are found throughout the

Objective	Fuel Costs	Emissions	Sum System Voltage Violation
Epsilon	0.1	0.001	0.001

TABLE II
USER-SPECIFIED EPSILONS FOR THE BORG MOEA

search, storing the best solutions in an offline archive. If the search has not found new boxes it is said to be “stagnated” and the search operators and population size are modified. Therefore, we visualize the search progress using “epsilon progress”, a timeseries of how many new epsilon boxes have been found. Asymptotic behavior of epsilon progress can be employed as a termination criterion for search.

Practically, epsilons act as a method for specifying the desired precision across the objective space. The epsilons used in the search are given in Table II and were selected based on the precision of the objective function coefficients given in Table I. Additionally, these precision values generally agree with the precision of reported solutions in the EOPF literature [3], [5]–[7].

An initial population of 100 was specified with a maximum of 20,000 function evaluations was specified for this search. Default parameter values were used for the remaining parameters which is justifiable given demonstrations of Borg’s excellent performance using its default parameterization [11], [12]. The parallelized version of Borg was run on a Dell OptiPlex 9020 desktop computer with an Intel Quad Core i7-4770 CPU with 16 GB of RAM.

C. Results

Figure 2 depicts the epsilon progress as the search unfolded. Using this visualization, we terminated the search at 20,000 function evaluations. The optimization took a wall time of roughly 30 minutes. It is worth noting that this wall time can be significantly reduced with increased computing power. Therefore, there is promise for implementing this algorithm for day-ahead planning in addition to long-term operational planning.

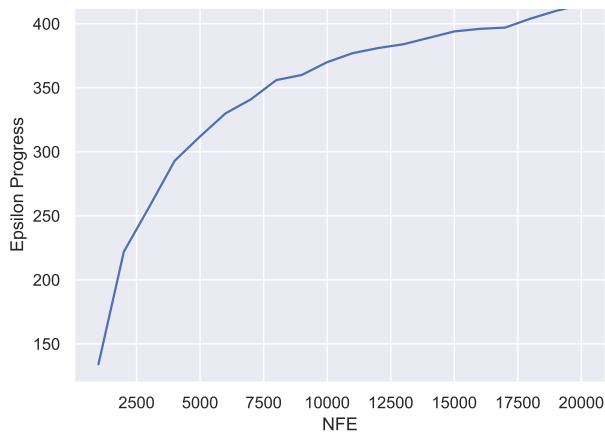


Fig. 2. Search progress. Abbreviations: Number of function evaluations (NFE)

Using the epsilons in Table II, the final tradeoff contains 50 solutions, with objective function values plotted in Fig. 3.

Because all objectives are minimized, an ideal solution would be a straight line across the bottom; crossing lines indicate tradeoffs among neighboring objectives. A three-cluster k-means clustering is depicted on the emissions objective to aid in viewing. One solution was selected as a “compromise” and shown in black. This solution was the only one that exceeded the 30th percentile for each objective.

The decision variable values of the solution set are depicted in Fig. 4, using the same k-means clustering color scheme. The plot shows the amount of active power produced by each generator, so unlike in Fig. 3, there is no special relationship for the ideal solution or crossing line.

Fig. 3 gives insight into system-wide performance. Generally, there is a tradeoff between cost and emissions as is evidenced by the conflicting green and blue solutions (i.e. solutions that have low emissions have a high cost and vice versa). This result is consistent with broader literature findings [3], [7], [9]. However, the voltage violation objective has allowed us to demonstrate alternative performance regimes. The orange solutions in Fig. 3 reflect tradeoffs between emissions and voltage violations. Many of these solutions would be dominated if only the cost and emission objectives were considered (i.e. other solutions have better performance with respect to *both* the cost and emission objectives). The solutions in this orange cluster have poor emissions and average cost performance but minimize the sum of system voltage violations.

Interactive visualization of tradeoffs such as in Fig. 3 could allow grid operators to apply acceptable limits or ranges of each objective value. In this fashion, the optimization objectives could be “converted” to hard constraints [13]. For example, a grid operator could filter solutions based on the criteria that the sum system voltage violation objective must be less than 0.08 (pu) and that emissions must be less than 0.0225 (ton/hr). This choice would eliminate half the green solutions and half the orange solution, and the grid operator could then see how the remaining solutions perform on the cost objective.

Fig. 4 lets us look at the tradeoffs between generators. A few clear regimes emerge with particular emphasis on generators five and six. Generally, solutions that have high emissions and low voltage violations result in high output at generator five and low output from generator six. Conversely, solutions that have low emissions and high cost do so by reducing power output at generator five and increasing power output at six. Such findings may not be easily determined from simply looking at the emission and fuel cost coefficients presented in Table I where we see that generators five and six are neither the cheapest nor the most-expensive generators.

An additional concern for grid operators would be *how* those violations are distributed throughout a grid. Simply put, one large voltage violation at a single bus has different operational impacts than many small violations across many buses, even though both cases may have the same system-wide sum of voltage violation. To this end, Fig. 5 depicts the statistical distributions of the voltage violations for each of the 50

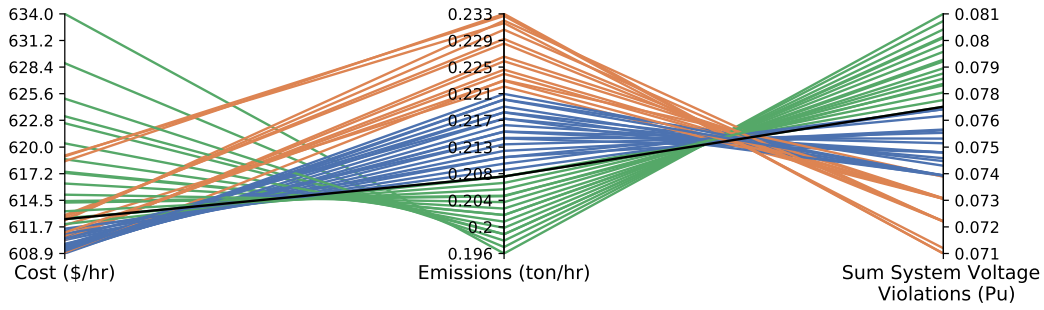


Fig. 3. Objective performance of nondominated solutions, where each line represents one possible solution. Because objectives are minimized, the ideal direction is downwards.

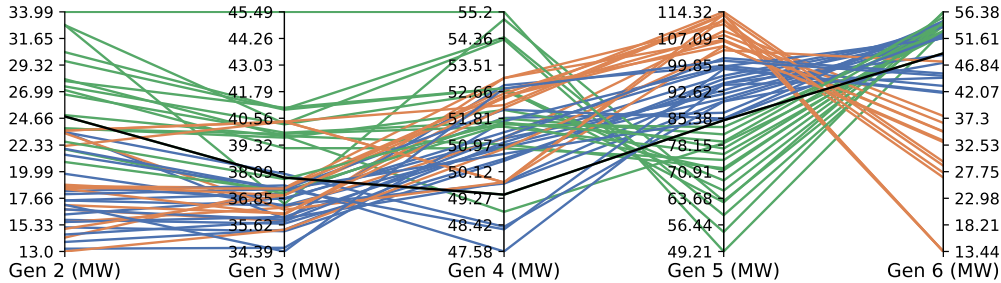


Fig. 4. Generator output decision variable values for the nondominated solutions.

tradeoff solutions. A kernel density estimate (KDE), a non-parametric estimator of a probability density function, is fit to each set of voltage violations for each of the 50 solutions and depicted in gray. Four of the solutions have been highlighted: the solution that minimized cost, emissions, and system-wide voltage violations as well as the compromise solution. The color of each of these four solutions is consistent with the clusters in Figs. 3 and 4.

From Fig. 5, notice the peak and tails of each KDE. Small and similar voltage violations would be depicted by a KDE with a high peak close to zero with narrow tails. In contrast, large voltage violations with a larger spread would be depicted with a peak much greater than zero with larger tails. It is important to note that any solution's KDE will integrate to one and therefore does not reflect the total system-wide voltage violations. To analyze a solution's system-wide voltage violation, see the sum system voltage violations axis in Fig. 3.

Comparing the distribution voltage violations for the minimum cost solution to the minimum emission solution, we see that the minimum cost solution's peak occurs at a larger value than the minimum emission solution's. Additionally, the minimum cost solution has heavier tails than the minimum emission solution. Therefore, we can conclude that the minimum cost solution produces voltage violations with greater variation than the minimum emission solution.

A similar comparison can be made between the compromise and minimum voltage violation solutions. The peaks of both of these solutions are comparable. However, there are clear differ-

ences in the tails. The minimum voltage violation solution has a heavier upper tail while the compromise solution has light tails. Again, this means that the minimum voltage violation solution produces a higher variation of voltage violations when compared to the compromise solution. Cross-referencing this information with Fig. 3, we see that the compromise solution has a far higher system-wide voltage violation than the minimum voltage violation solution. Therefore, the minimum voltage violations solution is able to obtain voltage violations by having higher voltage violations at a single bus whereas the compromise solution has many voltage violations of a smaller magnitude spread across more buses. As is evident by cross referencing Figs. 3 and 5, system operators can gain insights into both system-wide performance metrics as well as bus-level performance.

IV. CONCLUSION

This paper has presented a novel formulation of the EOPF problem where typical hard voltage constraints are considered an objective. This offline framework allows grid operators to tune allowable voltage violation levels before applying hard constraints to an online EOPF problem. This problem formulation was tested on the IEEE 30-bus system and the Borg MOEA was used to solve the problem. By considering the voltage violations as an objective instead of a hard constraint, the MOEA was able to find new solutions to the EOPF problem. Through state of the art visualization techniques, grid operators can quickly gain system-level insights into the tradeoffs between cost, emissions, and voltage violations,

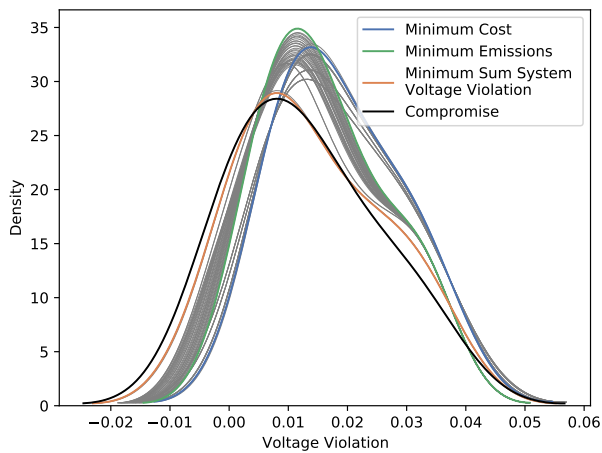


Fig. 5. Fitted kernel density estimates of voltage violations across all buses. Representative solutions are represented by the colored lines and appear in the legend. All other optimal solutions appear in gray.

and the sensitivity of objectives with respect to each other. Additionally, visualization techniques are proposed for gaining bus-level insights into the distribution of voltage violations within a network. This problem formulation allows operators to explore constraint design and objective sensitivity instead of specifying optimization preferences *a priori*. These results suggest that traditional formulations of the EOPF problem may limit the number of potential solutions, especially in cases where pre-specified voltage constraints may be flexible in practice. This work should not be used as a justification for ignoring voltage constraints altogether as prolonged voltage violations can have adverse effects in real-world systems [14]. This framework is not an explicit operating policy but is instead a tool to allow grid operators to make more-informed decisions when choosing an optimal solution for online EOPF problems. Readers are reminded that selecting among the nondominated policies is ultimately a question of engineering judgement.

Future research should conduct a more detailed study of the physical effects of violating voltage limits. It is likely that the consequences of exceeding voltage limits would differ among buses in a real-world system. Another possible problem formulation could constrain the voltages of certain critical buses while optimizing the excess voltages of other buses. The temporal and variability aspects of the real-world EOPF problem should also be investigated. Future work could perform a similar optimization over many timesteps with differing loads. It is likely the benefits of relaxing voltage constraints could be implemented during certain timesteps while allowing buses time to recover during other timesteps. System performance over many timesteps could be captured by performance-based metrics such as robustness, reliability, and vulnerability which are common in systems-level optimization literature [15]–[17].

ACKNOWLEDGMENT

This work acknowledges support by the U.S. Department of Education’s Graduate Assistance in Areas of National Need (GAANN) program under grant P200A180024. All supporting data and code are available at <https://osf.io/fd3mj/>

REFERENCES

- [1] EPA. Sources of greenhouse gas emissions. Library Catalog: www.epa.gov. [Online]. Available: <https://www.epa.gov/ghgemissions/sources-greenhouse-gas-emissions>
- [2] A. Farag, S. Al-Baiyat, and T. C. Cheng, “Economic load dispatch multiobjective optimization procedures using linear programming techniques,” *IEEE Transactions on Power Systems*, vol. 10, no. 2, pp. 731–738, 1995.
- [3] M. Abido, “A novel multiobjective evolutionary algorithm for environmental/economic power dispatch,” *Electric Power Systems Research*, vol. 65, no. 1, pp. 71–81, 2003.
- [4] K. Baker, G. Hug, and X. Li, “Optimal integration of intermittent energy sources using distributed multi-step optimization,” in *2012 IEEE Power and Energy Society General Meeting*, 2012.
- [5] R. King and H. Rughooputh, “Elitist multiobjective evolutionary algorithm for environmental/economic dispatch,” in *The 2003 Congress on Evolutionary Computation*, vol. 2, 2003, pp. 1108–1114.
- [6] V. Vahidinasab and S. Jadid, “Joint economic and emission dispatch in energy markets: A multiobjective mathematical programming approach,” *Elsevier Energy*, vol. 35, no. 3, pp. 1497–1504, 2010.
- [7] L. Wu, Y. Wang, X. Yuan, and S. Zhou, “Environmental/economic power dispatch problem using multi-objective differential evolution algorithm,” *Electric Power Systems Research*, vol. 80, no. 9, pp. 1171–1181, 2010.
- [8] D. Hadka and P. Reed, “Borg: An Auto-Adaptive Many-Objective Evolutionary Computing Framework,” *Evolutionary Computation*, vol. 21, no. 2, pp. 231–259, May 2013.
- [9] M. Abido, “Multiobjective evolutionary algorithms for electric power dispatch problem,” *IEEE Transactions on Evolutionary Computation*, vol. 10, no. 3, pp. 315–329, 2006.
- [10] L. Thurner, A. Scheidler, F. Schäfer, J. Menke, J. Dollichon, F. Meier, S. Meinecke, and M. Braun, “pandapower — an open-source python tool for convenient modeling, analysis, and optimization of electric power systems,” *IEEE Transactions on Power Systems*, vol. 33, no. 6, pp. 6510–6521, 2018.
- [11] D. Hadka and P. Reed, “Diagnostic assessment of search controls and failure modes in many-objective evolutionary optimization,” *Evolutionary Computation*, vol. 20, no. 3, pp. 423–452, 2012.
- [12] D. Hadka, P. M. Reed, and T. W. Simpson, “Diagnostic assessment of the borg MOEA for many-objective product family design problems,” in *2012 IEEE Congress on Evolutionary Computation*, 2012.
- [13] W. J. Raseman, J. Jacobson, and J. R. Kasprzyk, “Parasol: an open source, interactive parallel coordinates library for multi-objective decision making,” *Environmental Modelling & Software*, vol. 116, pp. 153–163, 2019.
- [14] American Society of Civil Engineers and Economic Development Research Group, “Failure to act: The economic impact of current investment trends in electricity infrastructure,” 2011.
- [15] T. Hashimoto, J. R. Stedinger, and D. P. Loucks, “Reliability, resiliency, and vulnerability criteria for water resource system performance evaluation,” *Water Resources Research*, vol. 18, no. 1, pp. 14–20, 1982.
- [16] M. Youssef, C. Scoglio, and S. Pahwa, “Robustness measure for power grids with respect to cascading failures,” in *Proc. of the Int. Workshop on Modeling, Analysis, and Control of Complex Networks*, 2011.
- [17] J. R. Kasprzyk, S. Nataraj, P. M. Reed, and R. J. Lempert, “Many objective robust decision making for complex environmental systems undergoing change,” *Environmental Modelling & Software*, vol. 42, pp. 55–71, 2013.